Electric Power Systems Research 220 (2023) 109341

Contents lists available at ScienceDirect

Electric Power Systems Research

journal homepage: www.elsevier.com/locate/epsr

Feasibility study and impacts mitigation with the integration of Electric Vehicles into Rwanda's power grid

Emmanuel Mudaheranwa [a,b,*], Hassan Berkem Sonder [a], Liana Cipcigan [a], Carlos E. Ugalde-Loo [a]

[a] School of Engineering, Cardiff University, Cardiff, UK
[b] Department of Electrical and Electronics Engineering, Integrated Polytechnic Regional College Karongi, Rwanda Polytechnic, Kigali, Rwanda

ARTICLE INFO

Keywords:
Distributed generation
Electric vehicles
Line loading
Loss and voltage analysis
Rwanda
Transformer loading

ABSTRACT

In recent years, fossil fuel transportation has grown significantly and Electric Vehicles (EVs) are essential to lowering transport-related pollution. This research uses the IPSA+ Power simulation tool to examine load-flow and establish Rwanda's power system's EV charging load capability. Rwandan grids with EV chargers are tested under various network reinforcement situations. According to simulation results, the maximum penetration rate that can be used to keep the Rwandan grid's operating characteristics within acceptable limits for registered private vehicles, buses, and taxis, is 1.5%, 10%, and 10%, respectively, if they are charged on 10 kW chargers. However, the permitted rates decrease to 1%, 8%, and 8% for these cars equipped with 20 kW chargers. This study suggested placing distributed generation units near important substations to reduce power losses and maintain busbar voltages within regulatory limits. Two of 18 transformers loaded above 80% with 10 kW charges. However, using 20 kW chargers, transformers at seven substations had loadings above 80%, with 83.7%, 83.9%, 82.3%, 88.2%, 87.6%, 84.7%, and 91.8%, respectively. A framework for regulating transformer loading was suggested, and it was shown that during peak demand, critical substations can contribute up to 6 MW to ensure that transformers operate at their highest possible level of efficiency. This study assumes the battery to charge to 70% and 30%. These regulations ensure drivers' comfort with their cars' SoC levels. Scenario 1 guarantees that electric vehicles will have the expected battery SoC levels, while Scenario 2 requires a little lower proportion to give the highest LRC. This is due to the fact that Scenario 2 is incapable of compensating for the change in power consumption while simultaneously executing real-time transformer and line loading regulation.

1. Introduction

As Road transport has been identified as the top contributor of greenhouse gas (GHG) emissions, resulting mainly due to an increased dependence on internal combustion engine cars across the globe. In its third National Communication Statement to the United National Action Plan on Climate Change, Rwanda's Ministry of Environment presented a variety of solutions for mitigating emissions, one of which was the implementation of EVs and fossil -based efficient systems [1,2].

The majority of Rwanda's road network consists of pavements that link the country's capital, Kigali, to the country's other main urban centres. There are also some roads in the country that are not paved; nevertheless, the nation's whole road network is scheduled to be completely repaved by the year 2025 [3,4]. The projections show that more than 150,000 passenger cars will be replaced by EVs by 2050 in the country [5]. As a result, by 2030, the total yearly electrical energy consumption for road transportation is expected to reach 100 GWh, and possibly even 500 GWh by 2050 (which is about 5% of the total demand) [6–8]. These estimates are thus increasing the need for a robust charging infrastructure and the government is seeking for viable policies and measures to facilitate the widespread use of EVs.

The operation of the transmission and distribution network will be significantly impacted by such a significant growth in the EVs deployment, causing steady state voltage drops, increase the power losses, and

Abbreviations: EV, Electric Vehicle; CPF, Continuation Power Flow; DG, Distributed Generation; GHG, Greenhouse Gas; LCE, Loading Control Error; LRC, Loading Regulation Capacity; PV, Photo Voltaic; REMA, Rwanda Environment Management Agency; RES, Renewable Energy Sources; RTDA, Rwanda Transport Development Agency; SOC, State of Charge; TLC, Transformer Loading Control; TLRF, Transformer Loading Regulation Framework; VOA, Voice of America; VSI, Voltage Sensitivity Index.

* Corresponding author.
E-mail address: mudaheranwae@cardiff.ac.uk (E. Mudaheranwa).

https://doi.org/10.1016/j.epsr.2023.109341
Received 18 July 2022; Received in revised form 21 January 2023; Accepted 14 March 2023
Available online 29 March 2023

overload distribution network equipment (such as lines and transformers), particularly when the charging coincides with the network's peak loading time [9,10]. Therefore, it is essential for the distribution network operators to make sure that the current energy infrastructure is capable of handling a major increase in the use EVs.

Even though there has been considerable progress in the existing literature to analyse the effect of EVs on test networks in other African countries (and across other continents of the globe), there is limited work assessing the feasibility of EVs and quantifying the effects of different charger techniques on real distribution networks with robust network control measures. This work analyses the grid-side challenges in Ruanda's power system associated with the connection of EVs and proposes solution and reinforcement method to assist the energy utility services in planning their networks and the generation in the future.

2. Literature review

This section summarizes the research published in the literature, including the novelty that this study aims to add, and the method that aims to bridge the research gaps.

In [11], the authors found that the electricity generation demand will increase between 12 and 23% if all the registered vehicles consume between 5 and 10 kWh on slow-speed chargers (< 10 kW) in the US. The research in [12] compared how the steady-state operating characteristics of a real distribution network is affected following the connection of 50 kW and 250 kW chargers and found that increasing the rating of chargers causes larger voltage drops and higher power losses near the charging point. The findings also demonstrated that the utilisation of a vehicle-to-grid (V2G) charger reduces the overloading on supply cables and improves the voltage profiles at the nearest busbars.

The integration of a DC charger during the peak loading hour of the network showed that the charger substantially increases peak demand and drops the voltage by up to 7% at the point of charging [13]. The cable that supplies the DC charging station was also critically overloaded during the peak loading hour. Other studies have analysed the impact of charging during peak periods on the transformer. In [14–16], it was demonstrated that a higher EV uptake would lead to greater transformer deterioration, and the increased temperature range would lead to transformer failure.

Different grid-side mitigation measures are proposed to reduce the impact of EV charging. In [17,18] the use of on-load tap changers and small-scale distributed generation (DG) units (in the form of solar and/or wind generation) near the congested substations and feeders improved the voltage profiles and reduced the transformer and cable losses in the high-voltage and medium-voltage (MV) distribution systems. In [19–23], charging EVs with local solar power was proposed to reduce losses and thermal impact, and improve power quality in the network. However, the utilisation of solar power requires a particular control framework and algorithm, as well as other economic considerations.

The study in [24] presents a new adaptive intelligent model predictive control (AIMPC) method for the frequency stabilization of a power plant that takes into consideration the SoC regulation of the battery of electric vehicles (EVs). In addition, a load frequency control (LFC) technique for a multi-microgrid (MMG) system that incorporates electric vehicles is proposed in [25] .The authors have not, however, taken into account the additional effects that EVs have on the other components of a power system. These include the loading of the transformer and the lines, as well as the voltage profile.

Other studies have shown the importance of renewable energy adoption in jobs creation. The research presented in [26] investigates whether or not Marshallian and Jacobean knowledge spillovers have an effect on the creation of jobs in the renewable energy sector. Through the use of data envelopment analysis (DEA), which is founded on the Malmquist productivity index, and tobit regression, the study investigates the production efficiency, as measured in terms of jobs and job spillovers, that has resulted from innovations in solar, wind, and renewable energy. The empirical data point to Jacobean externalities having no statistical impact on the job creation process, whereas Marshallian externalities appear to be negative.

The findings are extremely important for governments' efforts to build industrial policies for renewable energy, and they have strategic significance. In addition, through the utilization of the Input-Output analysis, the research presented in [27] sought to carry out an investigation into the possibility of financial investments being made in the energy sector in Italy. The findings demonstrated that investments in Renewable Energy Sources (RESs) have the potential to have a sizeable constructive effect on economies, particularly that of Italy, in both direct and indirect ways. Analyses of sensitivity revealed that the import proportion of key components of RES has a significant impact on occupational performance, particularly for PV systems.

There have been numerous studies in the Sub-Saharan region of Africa in the literature. [28] identified EVs as the most suitable low-carbon alternative for emissions mitigation pathway. The integration of a solar PV can also contribute to an effective raise in the exploitation of national energy resources, likely to result in consistent, cost effective, and durable energy access for the citizens in the country. The research in [29–31] addressed the technical and socio-economic concerns about EV uptake. The findings showed that EVs may be unaffordable for majority of the people in the Sub-Saharan region of Africa.

The literature review analysis has shown that, generally, the authors are developing load controllers at the transformer level, making decisions to transfer the load to other transformers or trip if the load is increased for protecting the transformer and lines. As a result of the tripping, the continuous power supply is interrupted, resulting in inefficiency and a decrease in network dependability and reliability [32]. The need to offer a control strategy that maximises the continuity of power supply while simultaneously lowering power losses and equipment failure is consequently imperative.

This work's primary contribution is to show that EVs may contribute significantly to the provision of useful flexibility services in the power system, rather than presenting a threat to grid stability or capacity. The main loading proposed mitigation measure involve the implementation of Transformer Loading Regulation Framework (TLRF) with the help of EV aggregators. The TLRF is effective at reducing line and transformer loading perturbations while maintaining the system loading percentage within acceptable limits.

3. Research elaboration

The grid that is under study, the research methods, and the data presentation are discussed in this section.

3.1. Power grid structure in Rwanda

The generation mix in the system is comprised of 29 hydroelectric power units that are interconnected, in addition to three plants that run on diesel. However, because of the high expenses of operation, backup generators (diesel-based) are only run during peak hours to make sure that the most possible use is made of hydroelectric power [33]. Around one third of the line is linked at the MV level, which includes substations at 30 kV, 17.32 kV, 15 kV, and 6.6 kV. The network under investigation is comprised of 32 substations, as presented in Table 1.

3.2. Modelling of networks with incorporated power generation plants

The IPSA+ Power computer software package, which is mainly designed to analyse the steady-state operational performance of electric power networks with a different loading flow condition, has been modified to include a model of the actual electric distribution system that is implemented in Rwanda. The generation mix in the system includes hydropower plants with a total power of 103.16 MW), and diesel-

Table 1
Substation data.

S/N	Input (kV)	Output (kV)	Apparent power (MVA)	Load (MW)	Load (MVAr)
		(kV)			
1	110	15	20	17.4	3.1
2	110	15	10	6.5	1.2
		30		8.8	3.6
3	110	30	20	8.3	2.9
4	110	15	10	7.4	1.5
5	110	15	10	4.5	0.9
6	110	15	10	9.8	1.5
7	110	15	20	0	0
8	110	30	2.5	1.7	0.175
9	110	30	3.15	2.4	0.15
10	6.6	30	5	2.1	0.25
11	6.6	110	20		
12	6.6	110	30		
13	110	15	45	28.8	4.8
14	110	30	10	8.6	0.5
15	110	30	1.5	0.9	0.14
16	110	30	6	4.3	0.84
17	110	30	10		
18	110	6.6	10		
19	30	6.6	5	3.4	0.7
20	6.6	30	10	7.8	1.56
21	30	6.6	5	3.3	0.66
22	30	6.6	6.6	4.8	0.9
23	110	30	1.6	1.1	0.2
24	110	15	2.5	1.8	0.26
25	30	6.6	1	0.4	0.072
26	30	6.6	1	0.44	0.081
27	30	6.6	1	0.51	0.09
28	30	6.6	5	3.2	0.63
29	110	15	20	0	0
30	110	30	2.5	1.7	0.175
31	110	30	3.15	2.4	0.15
32	6.6	30	5	2.1	0.25

based plants with a total power of 58.8 MW. However, due to the high operation costs, diesel-based power plants only operate during the peak hours to ensure the maximum use of hydro power. There are four PV power plants with a total installed and available capacity of 12.08 MW and 1.9 MW, respectively. Furthermore, the only peat fired plant in the country has a capacity of 15 MW and provides a power of up to 14.25 MW [34]. Lastly, there is also a methane-to-power plant with an installed capacity of 26.4 MW, which was commissioned in December 2015 [35,36]. Overall, the existing generation plants (including hydro, diesel, methane gas, biomass, and peat-to-power) in Rwanda can provide up to 222.9 MW [34].

IPSA (Interactive Power System Analysis) software is a modern and comprehensive power system analysis package for the design, planning and analysis of electrical networks. Using IPSA tool, Load flow calculations are performed using a fast-decoupled Newton-Raphson load flow technique that robustly handles both radial and meshed networks at all voltage levels [37].

Fig. 1 presents a simplified version of the network's structural diagram. After simulating the model using the IPSA+ software and then completing the load flow analysis, the authors were able to determine the influence that the integration of EVs would have on the load and voltage profile as well as the loading of the transformer. After the bus voltage has been estimated, it is then compared with the Rwandan voltage operation limits, which specify a minimum limit of 0.933 pu and a maximum limit of 1.044 pu. These values can be found in the Rwanda grid codes [33].

As part of the study investigation into the impact that electric vehicles (EVs) have had on the load profile, the study examines the computed load curve both before and after the introduction of EVs. The network consists of 32 substations denoted by numbers 1 to 32, connected at different voltage levels. Table 2 presents the data for the main substations without EVs.

Each substation is designated through S1 to S18 (real names have been anonymised due to confidentiality) in urban areas. The total base demand and generation from substations add up to 99.8MW and 87.4MW, respectively. It should be clarified that these specific urban-area substations are prioritised for EV connection to provide a realistic scenario for the Rwandan government wanting to increase the number of charge points in larger urban areas.

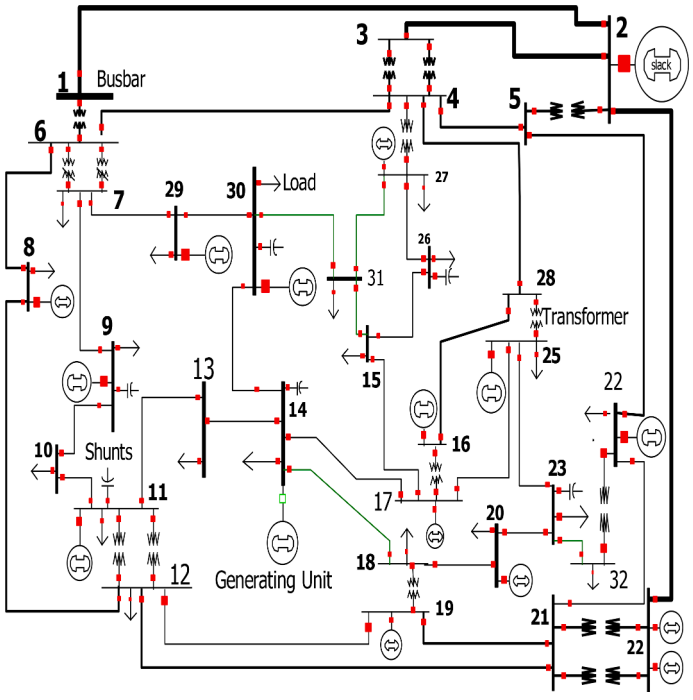

Fig. 1. The existing generation in the Rwanda power system.

Table 2
Demand and generation of suitable substations in base case.

S/N	Voltage (kV)	Rating (MVA)	Demand (MW)	Generation (MW)
1	15	20	3.5	13
2	15	10	1.2	2.4
3	15	20	13	0
4	15	10	7	25
5	15	20	7	0
6	15	10	5.8	11
7	15	20	3	0
8	30	2.5	2.1	0
9	30	3.15	8	7
10	30	5	3.4	0
11	30	5	0.6	0
12	15	45	4.8	4
13	30	10	2.5	0
14	30	1.5	6	0
15	30	6	1.2	0
16	6.6	5	4.7	0
17	30	10	2.5	25
18	6.6	6.6	3.5	0

3.3. Modelling and integration of EVs in the grid

During the load-flow analysis, each EV is represented as an unvarying voltage and power (CP-CV) model. The CP-CV recharging option is used to ensure that the grid receives steady power while the battery is being charged. Fig. 2 depicts an analogous battery model.

On the side that is connected to the grid, the electric vehicle charger receives the grid voltage (V_C), and while it is charging, it consumes the current (i_c), as depicted in the schematic diagram. V_{pack} and I denote the terminal voltage and the terminal current that is provided to the battery, respectively, on the battery side. The equivalent voltage of the battery is represented by the VOC_{-eq} symbol, and the resistance of the battery is represented by the R_{eq} sign.

The following functions are defined in relation to the CP-CV charging alternative that is being considered:

- Maintain Constant Power (CP): The power Pac remains constant, up till the maximum voltage of the battery is attained.
- Maintain a constant voltage (CV): The voltage Vpack remain constant, till the battery's state of charge (SOC) hits one hundred percent.

In accordance with [38–40], the battery's open circuit voltage (V_{oc}) and state of charge (SoC) can be computed. The model consists of a regulated voltage source denoted by V_{oc} connected in series with an impedance equivalent to that of a battery cell denoted by Ri. The value given by the letter V_t represents the voltage at the battery's terminals. The SOC is the only state variable represented by the model, and its derivation may be found in the following:

$$SOC = \frac{Q}{Q_{nom}} \tag{1}$$

However, if charging efficiency is neglected, the SOC change over time can be represented as:

$$\frac{dSOC}{dt} = \frac{i}{Q_{nom}} \tag{2}$$

The following formula can be used to represent the battery's open-circuit voltage, which is denoted by the symbol V_{oc}.

$$V_{oc}(Q) = V_o - \frac{K.Q_{nom}}{Q_{nom} - Q} Ae^{-(BQ)} \tag{3}$$

where

I is the charging/discharging current

Q represents the maximum throughput that is stored in the battery in Ah,

Q_{nom} represents the battery's rated capacity in Ah,

A represents the incremental zone magnitude in Volts,

B represents the incremental differential step response in Ah-1,

V_0 represents the battery voltage constant in volts, and K represents the polarization voltage (Volts).

The conventional method for determining the battery side power (P_{dc}) and grid side power (P_{ac}) is as follows:

$$P_{ac} = V_c \cdot i_c \tag{4}$$

$$P_{dc} = V_{pack} \cdot i \tag{5}$$

It follows from (3) that V_{pack} is related to the state-of-charge of the battery, which in turn makes P_{ac} related to the state-of-charge. So, (4) can be reformulated to be as follows:

$$P_{ac}(V_{pack}) = V_c \cdot i_c(V_{pack}) \tag{6}$$

And hence

$$P_{ac}(SOC) = V_c \cdot i_c(SOC) \tag{7}$$

$$P_{dc}(SOC) = V_{pack}(SOC) \cdot i \tag{8}$$

With the charger's efficiency (ρ) considered, the battery side power P_{dc} is calculated as:

$$P_{dc} = \rho P_{ac} \tag{9}$$

Considering (7) and (8) the current (i) is computed as follows:

$$i(SOC) = \rho \frac{V_c . i_c}{V_{pack}(SOC)} \tag{10}$$

Simulating the above equations, Figs. 3 and 4 present the results of a

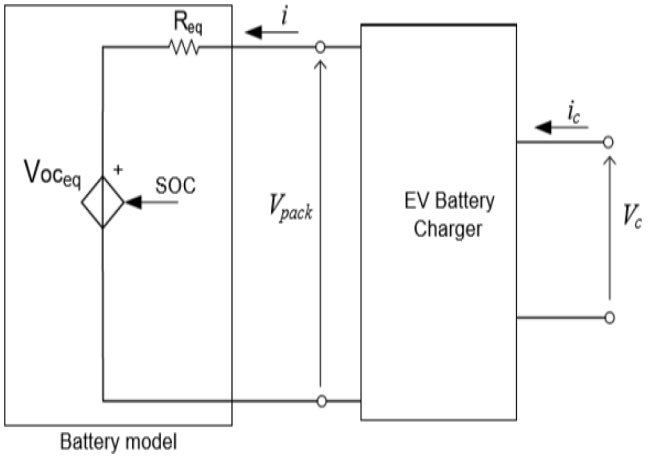

Fig. 2. Simplified schematic diagram of the EV batteries.

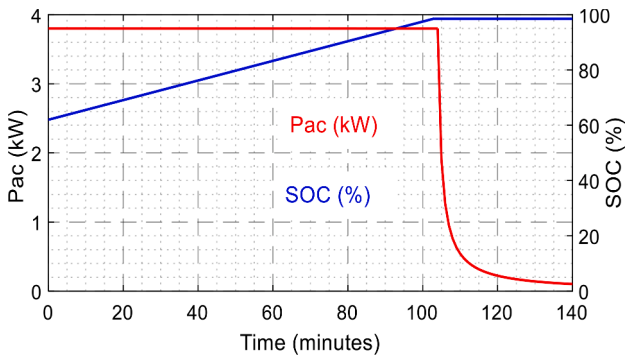

Fig. 3. Power and SoC profiles of the EV charger during CP-CV.

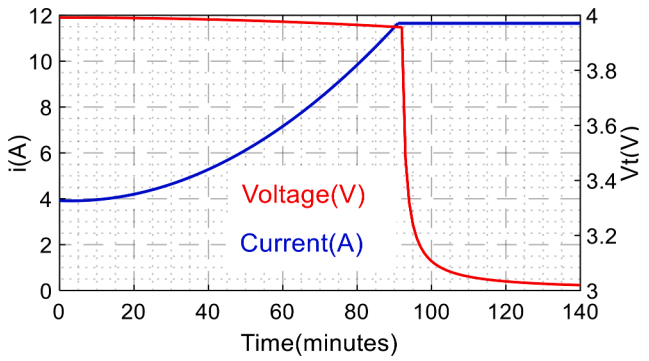

Fig. 4. Battery current and battery cell voltage during CP-CV.

simulation of the battery's characteristics.

At the beginning of the charging process, it is assumed that the battery had a starting SoC of sixty percent. It has been determined that the power output does not change until the voltage of the battery cell hits a predetermined threshold value of 4 V in this research. After reaching this stage, the charger will begin to transition into the CV mode.

3.4. EV connection scenario

In this work, the power demand of EVs is modelled based on the charging patterns and operation modes for different vehicle categories in Rwanda. These patterns represent daytime and night-time charging for private vehicles, buses, and taxis. The mode of operation for vehicle categories is shown in Fig. 5.

Using the traffic statistics from [1], and assuming that variance in driver behaviour represents the charging of various vehicle types, private owned vehicles are expected to charge between 00:00–06:00. Buses and taxis are considered shared mobility; therefore, buses' charging durations are extended by an additional charging period between 11:00–13:00 and 15:00–17:00, and 17:00–18:00 for taxis. It is critical to analyse the charging requirement of a particular vehicle at any time step to estimate the total power demand due to EVs' charging. The power demand of an EV battery being charged is parameterised in order to make numerical computations easier. The discrete quantities for the power demand during the recharging cycle are obtained in half-hourly periods from the curves illustrated in Fig. 4. Consequently, the respective charging power levels are denoted by (11).

$$S_i = \frac{S_{((i-1)\Delta t)} + S_{(i\Delta t)}}{2},\ i = 1, 2, \cdots m_c \tag{11}$$

where m_c denotes the total amount of half-hour time frames in the battery recharging process, i.e., 10 half-hour cycles as referred in Fig. 4, and Δt represents the time lapse while charging.

In this study, it is assumed that the initial charging time and the initial state of charge of the battery are two different elements that operate independently of one another. For this reason, the mathematical estimation of the mean value of the charging power at a specific time instant t is illustrated in (4) when a single battery is being charged.

$$\gamma(S) = \sum_{i=1}^{m_c} S_i \Psi(S_i, t) \tag{12}$$

where $\Psi(S_i, t)$ is the probability of EV charger load running at rated power S_i at time t ($1 \le t \le 24$). The probability density function (Ψ) is also given in (5).

$$\Psi(S_i, t) = \sum_{k}^{t} g(k) f\left(AptCommand2107_{;i-(t-k)}\right) \tag{13}$$

where $g(k)$ represents the probability of recharging initiated at time instant k ($k \le t$), and $f(AptCommand2107_{;i-(t-k)})$ is the probability that the first battery SoC will be at power level $S_{i-(t-k)}$. Eq. (6) can be used to approximate the SoC at the beginning of a recharging process $AptCommand2107_{;i}$ based on the average daily mileage, considering that the SoC of an EV decreases linearly with the distance travelled.

$$AptCommand2107_{;i} = \left(1 - \frac{\lambda d_d}{d_m}\right) \times 100\% \tag{14}$$

where λ represents the number of days the EV has travelled since the last charge, d_d and d_m represent the daily distance travelled by a vehicle and the maximum range of an EV, respectively.

In this paper, all EVs operate in CP-CV mode to represent simultaneous charging activities. As a result, a model that can represent numerous EV battery recharging loads at a given time instant is necessary. The model in this analysis is obtained by using the Central Limit Theorem for Sums [41–43]. According to this, if you continue to draw samples that are progressively larger and then add them all up, the sums of the samples will probably develop their independent normal distribution (the sampling distribution), which will become more similar to a normal distribution as the sample size increases. Therefore, the mean power demand of 'n' chargers equals $\sum_{j=1}^{n} \gamma_j(S)$; where $\gamma_j(S)$ represents the mean power demand of the j^{th} charger. Eq. (15) hence represents the total load when multiple EVs are being charged simultaneously.

$$P = \sum_{j=1}^{p} \sum_{i=1}^{m_c} S_i \cdot \Psi(S_i, t) + \sum_{j=1}^{b} \sum_{i=1}^{m_c} S_i \cdot \Psi(S_i, t) + \sum_{j=1}^{T} \sum_{i=1}^{m_c} S_i \cdot \Psi(S_i, t) \tag{15}$$

where P is the overall power demand for public vehicles, b is for buses, and T is for taxis.

3.5. Transformer and line loading mitigation

A novel method uses the deployed EVs into the network to support

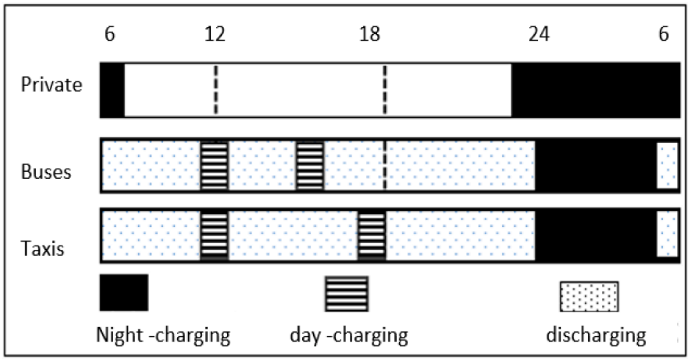

Fig. 5. Charging modes for different vehicle types.

transformer loading regulation process by introducing the TLRF with EV despatch by aggregators. While implementing this framework, the data of transformers (such as the power output, and maximum and minimum adjustment constraints) are uploaded to the central controller for determining the Loading Regulation Capacity (LRC) and having to perform the Transformer Loading Control (TLC). As a result of the Loading Control Error (LCE), the outputs of the transformers are altered in response to the notification from the central controller. This paper proposes a layered architecture during which EVs play a role within the TLRF. The schematic representation of the process is shown in Fig. 6. The framework is divided into four categories as indicated by colours: purple, green, light blue, and black. The LCE is detected at the Control Centre (purple category), and it is due to the power output and transformer loading deviance that are identified. Some of the LCE is shuffled to the aggregator in the LRC of EVs, with randomness involved. The regulatory distribution provided by the Central Controller is distributed to EV charging stations through the V2G deployment block in the EV Aggregator (green category). V2G can simply be defined as the technology that allows the stored energy of an EV to discharge it back to the grid for improving grid utilisation, meeting the excess demand and improve the reliability of utilities [44].

The 'Total LRC' block sums up all the LRCs that has been provided by the EV chargers. The V2G controller block is responsible for allocating the regulating duty to each EV at the EV Charging Station level (blue category), and the required power to charge is maintained instantaneously to guarantee that EVs achieve the intended SoC percentage. The 'Interface Circuit' block is responsible for communicating with individual EVs on behalf of the 'Telemetry Management System' block. It regulates the charging and discharging of an EV in response to the information provided by an EV charger, and thereafter sends the information on EVs (such as the battery SoC, the plug-in duration, and the expected battery SoC) in real time. The dynamics of the framework process is explained in more detail as follows

3.5.1. EV despatch in the control centre

Eq. (8) describes the LCE that EVs undertake in the network.

$$LRC_{t+1}^{dispatch} = f(LCE) \tag{16}$$

It depicts the dispatching from the central controller to EVs throughout their LRCs. The function that represents LCE can be affected by renewable energy integration, generating unit reserves, the LRC of EVs, and a variety of other conditions. Therefore, (8) is generally undetermined, and hence can be determined by introducing a random variable 'R' and other regulation limits (such as up limit regulation and down limit: (LRC_k^{up}, LRC_k^{down}, respectively) by the aggregator. To explicitly describe this uncertainty, (8) is rewritten as shown in (9).

$$f(LCE) = R.\begin{cases} -min\left(|LCE|, LRC_t^{up}\right)\ LCE \le 0 \\ min\left(LCE,\ LRC_t^{down}\right)\ LCE > 0 \end{cases} \tag{17}$$

Since the despatch is uncertain, the probability that R will follow is estimated by using non-parametric probability distribution estimation as in [45,46].

3.5.2. Despatch control in EV aggregator

The LRC for an EV aggregator is obtained by adding the LRCs of each individual EV charger for the aggregator ($LRC_{j,t+1}^{up}$, $LRC_{j,t+1}^{down}$), and it can be calculated according to (10).

$$\begin{cases} LRC_{t+1}^{\text{up}} = \sum_{k=1}^{\text{p}} LRC_{j,t+1}^{\text{up}} \\ LRC_{t+1}^{\text{down}} = \sum_{k=1}^{\text{p}} LRC_{j,t+1}^{\text{down}} \end{cases} \tag{18}$$

In an EV aggregator, the regulatory task that has been assigned by the central controller is to be dispersed to every individual EV in the studied network. The regulatory duty that has been assigned to every EV is proportional to the LRC that has been uploaded to it.

$$LRC_{j,t+1}^{\text{station}} = \begin{cases} LRC_{t+1}^{dispatch} * \dfrac{LRC_{j,t+1}^{\text{up}}}{LRC_{t+1}^{\text{up}}}, (LRC_{t+1} \le 0) \\ LRC_{t+1}^{dispatch} * \dfrac{LRC_{j,t+1}^{\text{down}}}{LRC_{t+1}^{\text{down}}}, (LRC_{t+1} > 0) \end{cases} \tag{19}$$

The LRC of an EV charging station at time $t + 1$ is determined according to (12).

$$\begin{cases} LRC_{j,\ t+1}^{\text{up}} = \sum_{i=1}^{NJ} S_{i,t}^{\text{up}} \\ \qquad\qquad (j = 1, \ldots, J) \\ LRC_{j,t+1}^{\text{down}} = \sum_{i=1}^{Nj} S_{i,t}^{\text{down}} \end{cases} \tag{20}$$

where Nj is the total number of EVs deployed in the charging station number j, $S_{i,t}^{up}$ is the up regulation of an EV at time t, and J is the EV station deployment.

$$\begin{cases} S_{i,t}^{\text{up}} = S_{\max} + S_{i,t} \\ S_{i,t}^{\text{down}} = S_{\max} - S_{i,t} \end{cases} \tag{21}$$

S_{max} : maximum power charger, and $S_{i,t}$, the power of the battery at time t.When the demand for electricity (P_{dem}) is higher than the capacity of the charging station's nominal transformer (P_{Tx}), the utilization of already-deployed EVs can help minimize the amount of power that is coming into the station. This prevents the transformer from becoming overloaded, which happens depending on the amount of power supplied from EVs. Fig. 7 illustrates the regulation of EVs for the purpose of

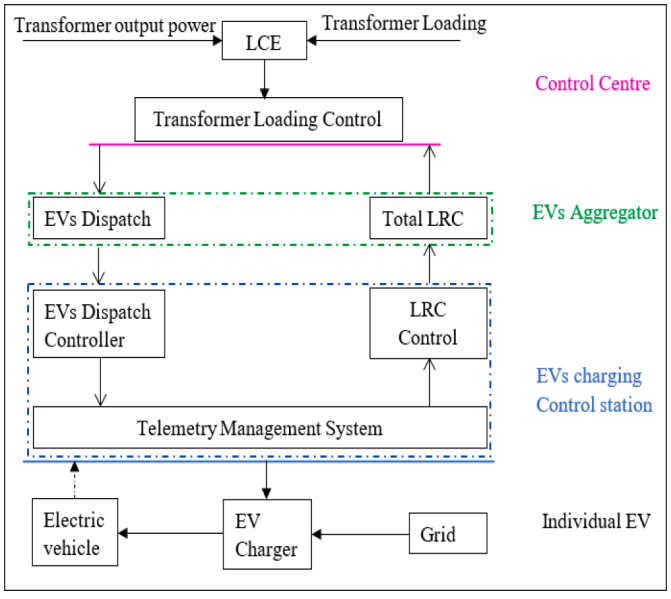

Fig. 6. Hierarchical framework for deployment of EVs in TLRF.

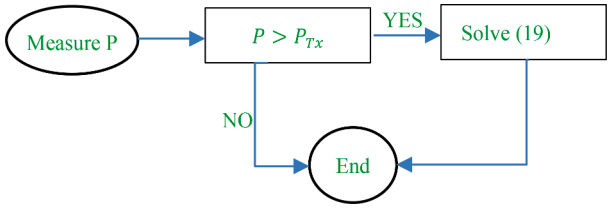

Fig. 7. Simplified flow chart for transformer overloading regulation with EVs.

reducing transformer overloading. When the EV load demand is more than the transformer's nominal capacity, the EVs' contributed power is computed in accordance with (21). As long as the battery SOC restrictions are met, the EVs will keep on supplying the necessary amount of energy.

It is important to note that even though there is only one point of power connection, there is always the potential to either export or import electricity at any particular instant. In the event that it is necessary, electric vehicles can be engineered to enable transformer loading regulation. Fig. 8 depicts the aggregated control procedure for the overloading of the transformer as well as the charge of the batteries. It is absolutely necessary to ascertain the transformer's nominal rating before making any decisions regarding the appropriate size of EVs. The load demand profile of the chosen area, which is depicted in Fig. 12, demonstrates that load demand is relatively high for a specific period of the day. According to this illustration, overloading the transformers between the hours of two in the afternoon and eleven o'clock at night can be readily prevented.

4. Results and discussions

Simulation findings from different case studies are presented and discussed in this section.

4.1. EV charging scenarios

With the help of the IPSA+ software tool, a variety of situations and case studies are modelled and investigated. Calculated and converted to represent the penetration rate for the transportation sector in Rwanda for the year 2022, the total number of registered cars for private vehicles, buses, and taxis is derived from the data on transport found in [47]. Table 3 is a presentation of these figures.

Rwanda's registered petrol-powered automobiles as of 2022 are shown in the data. Taxis account for the least percentage of all cars, with private automobiles accounting for the majority. Two charging scenarios are considered for simulation cases in addition to no EV scenario.

Table 3
Variety of fuelled cars in Rwanda.

Vehicle Type	Total	Rate of Penetration (%)
Private cars	107,787	91.7
Buses	5185	4.5
Taxi	4289	3.8
Total	117,256	100

The selection of the scenarios is based on the fact that this will be the first time that EVs are adopted and on the fact that the existing infrastructures are likely to support low power rated chargers. These types of chargers are classified as slow charging and the maximum power rating is 20 kW. The authors will not be picking any of the other possible types of electric vehicle chargers, which include the technology for rapid charging (up to 50 kW), or high-speed charger (up to 250 kW) because this will be implemented only once the network infrastructure is strengthened. The slow chargers were the first type of electric vehicle (EV) charger, and it is ideal to use when you have a good deal of free time. The charging mode for various vehicles is shown in Fig. 5, and it reveals that the majority of the vehicles have a lot of time to be charged. In this regard the normal charging method is selected.

The selected scenarios are as follows:

- Scenario 1: All EVs are charged using 10 kW chargers
- Scenario 2: All EVs are charged using 20 kW chargers

The number of EVs that are connected to 18 substations in the network is equal for both scenarios; however, the total demand due to charging is larger in Scenario 2 due to higher-power chargers (e.g., 20 kW). In addition, the total number of registered cars to be replaced with EVs are also calculated and shown in Table 4 for each scenario.

When it comes to total demand, electric vehicle charging at 10 kW and 20 kW stations consume 27 MW and 45 MW, respectively. The next

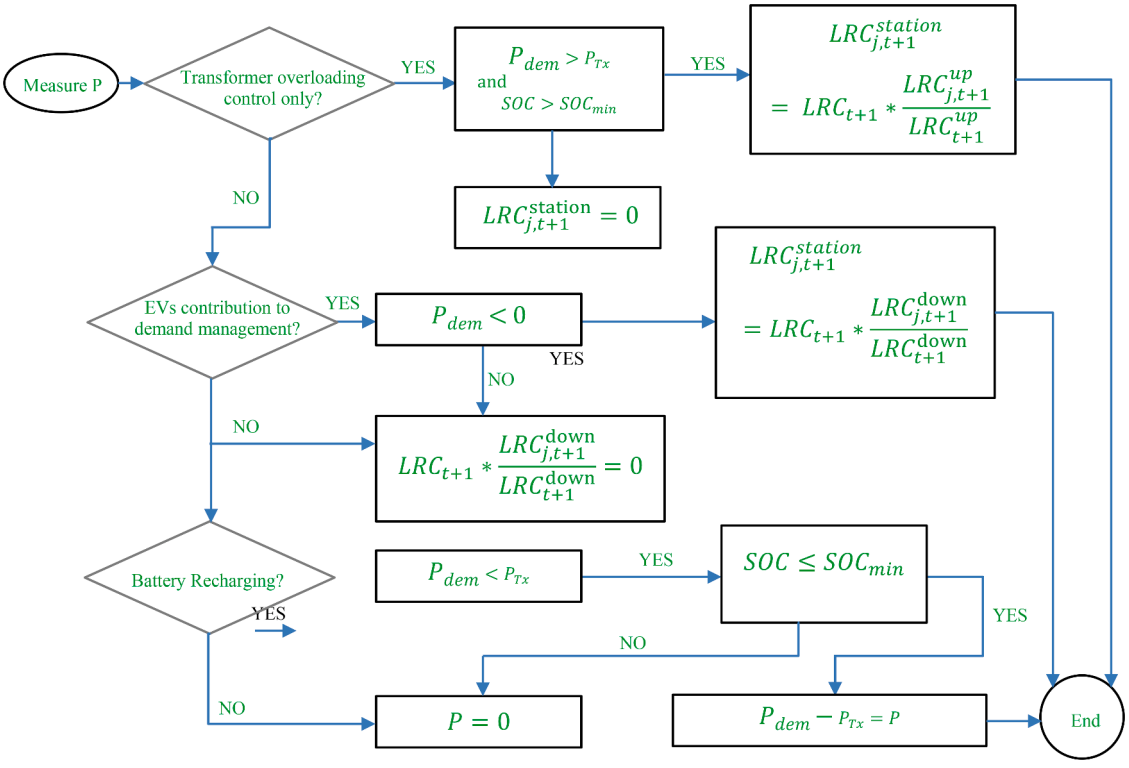

Fig. 8. Flowchart for the proposed transformer loading control framework with the participation of EVs.

Table 4
Distribution of vehicles for both scenarios.

Scenario	EV Penetration (%)			Charging Demand (MW)
	Private Cars	Buses	Taxis	
Scenario 1	1.5	10	10	27
Scenario 2	1	8	8	45

subsections contain an analysis of the effects that these potential outcomes could have.

4.2. Impact on distribution voltage stability

At the distribution side in Rwanda, the voltage requirements should be kept within the permitted levels of 1.044 p.u. and 0.933 p.u. respectively. Fig. 9 presents the findings on the voltage profile.

According to the findings, most of the busbars experience voltage fluctuations once 10 kW and 20 kW chargers are connected to the network. At substations 3 and 18, where voltage drops the least, and at substations 10, 12, and 16, where voltage drops the most, the difference in voltage is at its greatest. Despite this, the voltage continues to fall within the parameters set by the regulatory body.

4.3. Impact on load profiles

The charging demand for both scenarios after the connection of EVs is shown in Fig. 10.

The daily consumption pattern of electric vehicles reveals a maximum demand of either 27 MW or 45 MW, depending on which scenario is being considered. Since it is expected that charging events take place during the night, the peak demand for charging takes place between the hours of 23:00 and 03:00 in both of these situations. Between the hours of 07:00 and 11:00 and 15:00 and 19:00, the minimum demand for charging is approximately 1.2 MW and 1.8 MW, respectively, for Situations 1 and 2.

Each car type adds to the required power of EVs in proportion to the time it takes to charge. For example, as shown in Fig. 11, private cars contribute significantly to power demand (approximately 70%) between 02:00–04:00 and 20:00–23:00, whereas bus peak demand contributions reach a maximum of 60% between 11:00–13:00 for both scenarios.

The effect of EVs charging on the total base network demand is presented in Fig. 12.

According to the findings, the increased power consumption caused by EVs does not impact the shape of load demand curves for the basic scenario; however, it does affect the size of peak demand significantly. This is due to the fact that EVs have a lower peak demand. During the late hours of the night (that is, between the hours of 19:00 and 02:00),

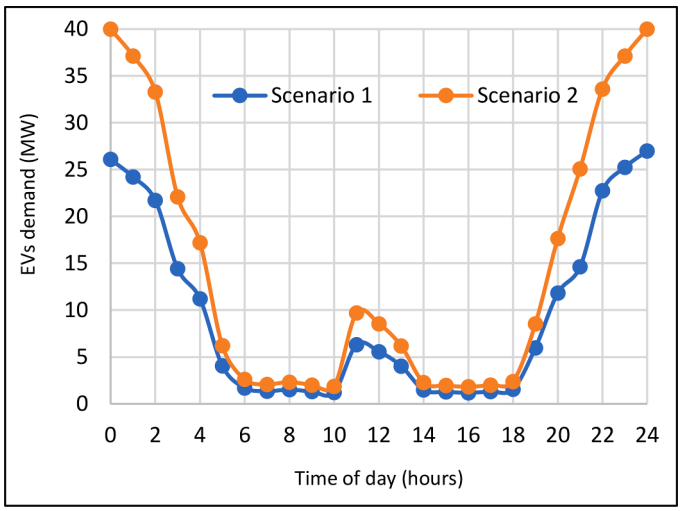

Fig. 10. EV demand profiles for Scenarios 1 and 2.

the total demand on the network increases from 100 MW to 180 MW. In addition, demand for Scenarios 1 and 2 stays rather consistent with that of the baseline scenario during the other hours of the day.

4.4. Sizing and placement of distributed generation units

Simulation results have demonstrated that simultaneous charging is a challenge for the energy providers in Rwanda. For this reason, two DG units are proposed to be connected near the critical substations with EVs in this study.

The findings of the simulation showed that connecting DG units in densely populated and congested locations made it easier to connect EV chargers and improved voltage profiles by 1–3 percent. In addition to this, as of the year 2022 [48]. However, the losses are recorded as 22% during base case scenario in this study. Overall, total network losses were higher in Scenario 2 due to larger demand of EV charging. Load-flow analysis shows the network losses of 53.4 MW, and 58.2 MW in Scenario 1, and Scenario 2, respectively. As a results, the addition of 6.5 MW and 24.5 MW DGs during the first and second scenario, reduced the network losses down to 46.9 MW and 47.9 MW, respectively which resulted in the improved voltage profile as discussed before. Continuation Power Flow (CPF) tool for analysing the steady state voltage stability is used to optimally determine the sizing and placement of DGs to support congested substations [49]. Two performance indices are used:

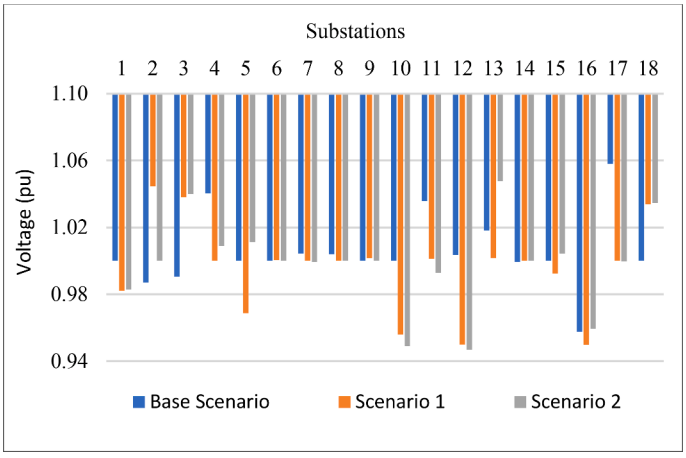

Fig. 9. Substation voltage profiles for all scenarios.

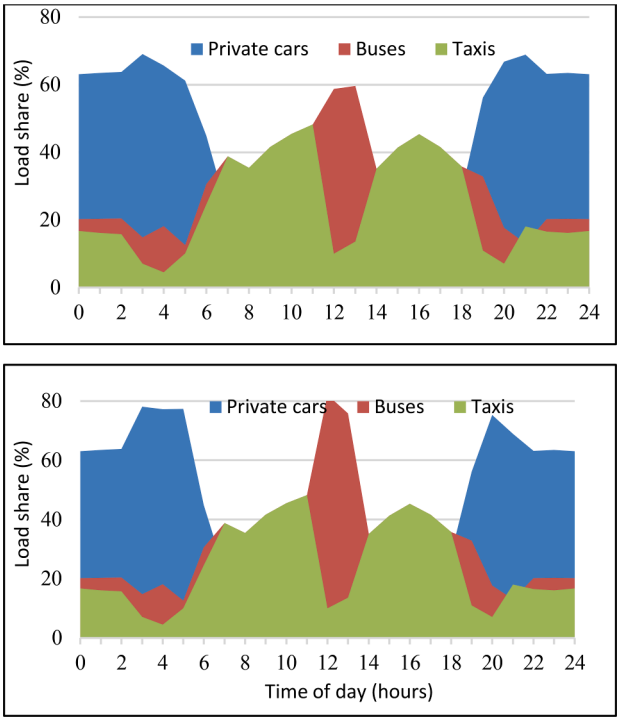

Fig. 11. Demand shares for each type of vehicle, expressed as a percentage. (Top: Scenario 1, Bottom: Scenario 2).

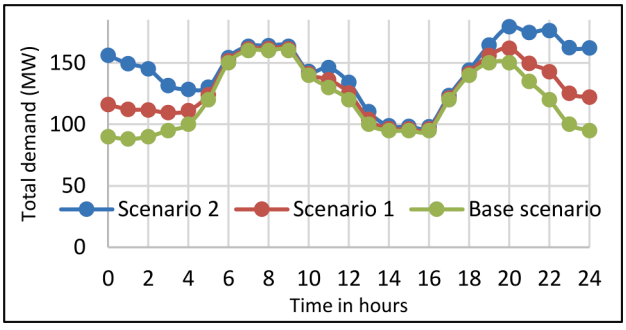

Fig. 12. Total demand for each scenario.

4.4.1. Active and reactive power loss

These indices help in analysing the impact of DGs on active and reactive power losses. Eqs. (14) and (15) are used to determine these, respectively.

$$AP_{LI} = \left(\frac{P_{Loss} - P_{Loss}^{DG}}{P_{Loss}}\right) \times 100\% \tag{22}$$

$$RP_{LI} = \left(\frac{Q_{Loss} - Q_{Loss}^{DG}}{Q_{Loss}}\right) \times 100 \tag{23}$$

where AP_{LI} *and* RP_{LI} represent the active power losses indices and reactive power losses indices, respectively. Loss indices should be higher when the DG is placed in the most optimal location.

4.4.2. Voltage sensitivity index

The Voltage Sensitivity Index, also known as VSI, provides a direct indicator of the maximum bus voltage deviation at the point when the voltage collapses. The bus in the system that has the greatest VSI has been determined to be the "weakest" point in the system. The following is how the VSI value for bus k is calculated: The VSI for bus '*k*' is determined as follows:

$$VSI_k = \frac{V_k^{base} - V_k^{critical}}{V_k^{base}} \tag{24}$$

where V_k^{base} and $V_k^{critical}$, are the acceptable maximum voltage limit and voltage at bus *k*, respectively.

4.5. Impact on distribution lines and transformers

The loading of transformers for 18 substations is shown in Fig. 13. Table 5 shows the loading on the power lines.

With the usage of 10 kW chargers, the loading on two of the transformers exceeded 80% (i.e., transformers at substations 11 and 16 with 81.6% and 91%, respectively). With the usage of 20 kW chargers, seven transformers at substations 1, 5, 7, 10, 12, 13, and 16 are overloaded with recorded exceeding of 83.7%, 83.9%, 82,3%, 88,2%, 87.6%, 84,7%, and 91.8%, respectively. Transformers at substations 10, 12, and 16 were severely overloaded (over 85%) in Scenario 2. Continuous loading on those substations would reduce their life-time expectancy, as also shown by other studies in the literature [50–54].

According to the results quantifying the loading effect on the lines, it can be seen in Table 5 that the loading on 10 branches is between 65 and 70% (which is a safe limit). However, eight other branches are significantly subjected to critical conditions and their ratings are exceeded by up to 70–85%. As a result, this can be the cause of worsened network reliability and security, as also investigated by other studies in the literature [55,56].

4.6. Transformer and line loading regulation framework

When EVs are used to regulate transformer and line loading, it has been demonstrated that the TLRF is more effective in lowering the LCE because there is more power available to increase the LRC. The total calculated LRC at each substation is shown in Fig. 14. According to the results in Fig. 14, it is evident that the total loading regulation power obtained after the application of the proposed method is sufficient to meet the total demand of the 18 substations with 10 kW and 20 kW chargers, where during peak demand it can add up to 6MW at the critical substations.

The behaviour of a randomly selected EV battery is shown in Figs. 15 and 16 during charging and discharging, respectively. When conducting an analysis of the limitations that are necessary to contribute to the regulation of the transformer's loading, both the charging and discharging characteristics are taken into consideration. The primary objective is to determine whether or not it is feasible, after charging the vehicles, to achieve a state of charge (SoC) of 70% for a transformer loading regulation capacity (TLRC) that will compensate for loading

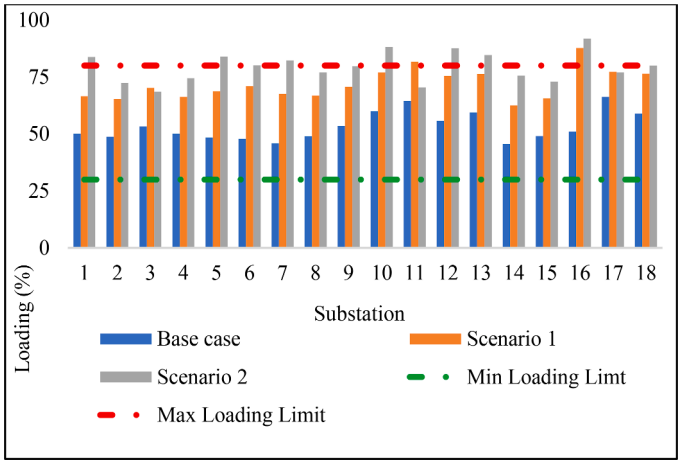

Fig. 13. Transformer loading expressed in percentage (%).

Table 5
Line loading for selected branches.

Branches		Line loading%		
From bus	To bus	Base case	Scenario 1	Scenario 2
1	2	63.2	66.6	73.8
1	6	61.9	65.3	72.4
5	2	66.4	70.3	78.6
2	3	63.1	66.3	74.4
3	6	61.5	68.8	85.9
8	12	60.9	71	80.1
10	9	58.9	67.5	88.3
10	11	61.9	66.9	77
7	9	66.5	70.7	79.7
7	6	73	77.1	88.2
7	8	77.4	81.6	90.4
26	15	68.7	75.5	87.6
14	17	72.4	76.3	84.7
5	4	58.6	62.5	75.6
4	3	62	65.6	73
4	3	64.1	67.7	81.8
4	6	79.3	85.4	98.3
11	12	72	76.4	91.5
11	18	61.2	65.2	73.9
17	16	61.8	65.8	81.9
18	15	61.5	66.6	78.1

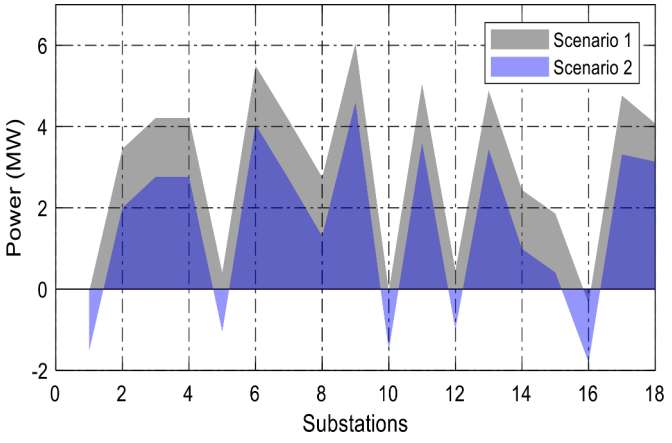

Fig. 14. Total loading regulation power at critical substations (positive: grid contribution, negative: EVs contribution).

control error (LCE).

It is assumed that each EV's battery SoC status is measured after an interval of time for battery discharge and instantaneously monitored during charging period. It is required that a given number of EVs will be disconnected from the charger when the information about required power to regulate the loading of transformer is received. In this regard, it is possible that some EVs will be at the SoC levels that are below, over, or equal to the predetermined SoC level (in this study upper limit 70%, and lower limit 30%). To measure and monitor the battery SoC levels, the battery model presented in (10) is used to simulate the battery behaviours where it is further extended as in (25) to include the change of the EV battery energy.

By considering the change in energy of the EV battery, the SoC levels are expressed as:

$$\mathrm{SOC_i} = \mathrm{SOC_i^{start}} \pm \frac{1}{E_i^{nominal}} \Delta E_i \tag{25}$$

where,

$\mathrm{SOC_i^{start}}$ represents the initial battery's SoC.

$E_i^{nominal}$ denotes the rated energy of the battery, and

ΔE_i is the energy change during charging or discharging period of the battery and satisfies:

$$\Delta E_i = \int_0^T P_i(t)dt \tag{26}$$

where,

T is the plug in / discharging period

The maximum and minimum battery SoC of 70% and 30% have been assumed, respectively. These limits were chosen to ensure that the drivers are confident with the SoC level of their vehicles. According to Figs. 15 and16, Scenario 1 guarantees the expected battery SoC levels of

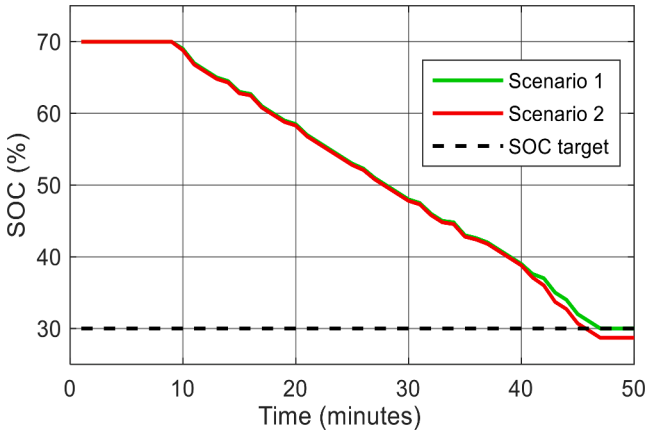

Fig. 16. Discharging behaviour of the EV battery.

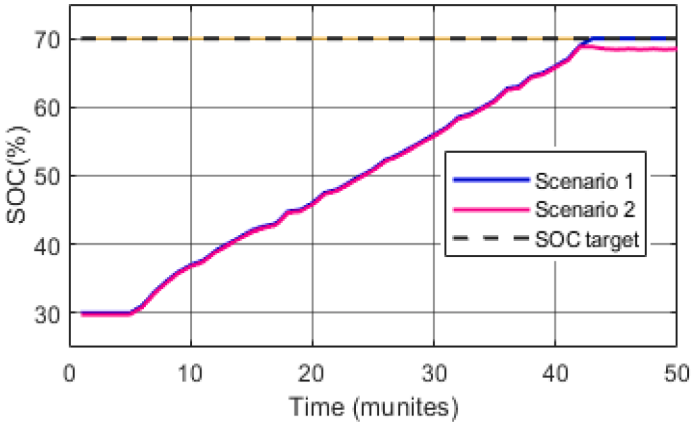

Fig. 15. Charging behaviour of the EV battery.

EVs, while the Scenario 2 requires the battery SoC to be slightly below the required percentage to provide the maximum LRC. This is because while implementing real-time transformer and line loading regulation, Scenario 2 cannot recompense for the change in power consumption.

5. Conclusion

This In this study, which used a realistic modelling approach, the integration of several types of electric vehicles (EVs) into Rwanda's transportation and electrical networks was analysed. The EVs were modelled around the existing traffic pattern in Rwanda, which was taken into consideration. According to the findings, electric vehicles can only make up 1.5 percent, 10 percent, and 10 percent of the total number of privately registered automobiles, buses, and taxis, respectively, if the charging stations are 10 kW. Chargers with a capacity of 20 kW bring down the maximum allowable uptake level for their respective modes of transportation to 1 percent, 8 percent, and 8 percent, respectively.

Findings from simulations have shown that the shift in load demand that may result from the introduction of electric vehicles (EVs) could result in the introduction of new peak loads within the network. This may result in voltage drops and increased power losses in urban areas where larger commercial and/or industrial customers are connected alongside EV chargers. The findings of the simulation also showed that the inclusion of 10 kW chargers in 18 separate substations is not conceivable unless DG units are connected near crucial spots. It should be made clear that the number of DGs, as well as their size, can be expanded in proportion to the growth in the number of EV charges.

In Rwanda, the total network losses are around 19.1% [57]. The losses were recorded as 23% during base case scenario in this study. Overall, total network losses were higher in Scenario 2 due to larger demand of EV charging. Load-flow analysis has shown that network losses were 53.4 MW, and 72.4 MW in Scenario 1, and Scenario 2, respectively. The addition of a 6.5 MW and 24.5 MW DGs during the first and second scenario reduced the network losses down to 46.9 MW and 47.9 MW, respectively.

The analysis on the loading of transformer with the optimal power flow showed that some parts of the network are overloaded with 10 kW and 20 kW chargers.

Considering the transformer loading it was found:

- With the usage of 10 kW chargers, the loading on two amongst the 18 considered transformers exceeded 80%.
- With the usage of 20 kW chargers, transformers at seven substations were found to have a loading exceeding 80%, with the recorded loading 83.7%, 83.9%, 82,3%, 88,2%, 87.6%, 84,7%, and 91.8%, respectively.

It was proposed a framework for regulating the transformers loading and it was demonstrated based on this framework that during peak demand a capacity of up to 6 MW at the critical substations can be added to guarantee that the transformers function at their highest possible level of efficiency.

Researchers have assumed that the battery will have a maximum and minimum state of charge of 70% and 30%, respectively. These restrictions were decided upon to make sure that drivers are comfortable with the SoC levels of their respective automobiles. According to the findings, Scenario 1 ensures that electric vehicles will have the battery SoC levels that were anticipated, whereas Scenario 2 mandates that the battery SoC be somewhat lower than the required percentage in order to deliver the highest LRC. This is due to the fact that Scenario 2 is incapable of compensating for the change in power consumption while simultaneously executing real-time transformer and line loading regulation.

CRediT authorship contribution statement

Emmanuel Mudaheranwa: Conceptualization, Methodology, Software, Data curation, Writing – original draft. **Hassan Berkem Sonder:** Writing – review & editing. **Liana Cipcigan:** Supervision. **Carlos E. Ugalde-Loo:** Supervision.

Declaration of Competing Interest

The authors declare that they have no known competing financial interests or personal relationships that could have appeared to influence the work reported in this paper. The authors have no affiliation with any organization with a direct or indirect financial interest in the subject matter discussed in the manuscript.

Data availability

Data will be made available on request.

Acknowledgement

This work was supported by DT E Network+, funded by EPSRC, grant reference EP /S032053/1. The authors would like to use this opportunity to extend their heartfelt appreciation to the Energy Group in Rwanda for supplying the information that was required. Of addition, the author would like to express their gratitude to the Commonwealth Scholarship Commission in the United Kingdom for providing sponsorship.

References

[1] E. Mudaheranwa, H.B. Sonder, L. Cipcigan, Feasibility study and impacts of EV penetration in Rwanda's MV distribution networks, in: 6th IEEE International Energy Conference, ENERGYCon 2020, Sep. 2020, pp. 284–289, https://doi.org/10.1109/ENERGYCon48941.2020.9236568.
[2] REMA, "Third national communication under the united nations framework convention on climate change," 2018. [Online]. Available: www.rema.gov.rw.
[3] F. Year, "02 Coaches manual annual report RTDA," 2019.
[4] African Development Bank Group, "Rwanda transport sector review and action plan," 2015.
[5] Eugene, Uwimana, Rwanda encourages youth to use electric motorcycles. Voice of America, August 2019. Available: https://www.voanews.com/a/africa_rwanda-encourages-youth-use-electric-motorcycles/6174393.html (accessed Nov. 10, 2021).
[6] REMA, "Rwanda environment statistics compendium final report," 2019.
[7] Ministry of infrastructures, "Republic of Rwanda Energy Sector Strategic Plan 2018/2019-2023/2024," 2018.
[8] E. Mudaheranwa, G. Masengo, Y.O. Odoakah, L. Cipcigan, and C.E. Ugalde-Loo, "Development of Rwanda's future energy scenarios for long-term investment and planning," *2021 3rd Asia Energy and Electrical Engineering Symposium, AEEES 2021*, pp. 1124–1129, Mar. 2021, doi: 10.1109/AEEES51875.2021.9403043.
[9] Ministry of Infrastructure (MINENFRA), "Forward looking Joint Sector Review (JSR) report for fiscal year 2021/22 Energy sector," Kigali, 2021.
[10] Rwanda Transport Development Agency, Manual Annual Report RTDA, Kigali, 2018.
[11] C. Yang, R. McCarthy, Electricity grid impacts of plug-in electric vehicle charging, EM: Air Waste Manage. Assoc. Magaz. Environ. Managers (JUN) (2009) 16–20.
[12] H.B. Sonder, L. Cipcigan, C.E. Ugalde-Loo, Voltage analysis on MV/LV distribution networks with the integration of DC fast chargers, in: 6th IEEE International Energy Conference, ENERGYCon 2020, Sep. 2020, pp. 260–265, https://doi.org/10.1109/ENERGYCON48941.2020.9236619.
[13] H.B. Sonder, L. Cipcigan, and C.E. Ugalde-Loo, "Integrating Dc Fast/Rapid Chargers in Low Voltage Distribution Networks," pp. 59–65, 2021, doi: 10.1049/icp.2021.1251.
[14] A. Amin, et al., A review of optimal charging strategy for electric vehicles under dynamic pricing schemes in the distribution charging network, Sustainability (Switzerland) 12 (23) (2020) 1–28, https://doi.org/10.3390/su122310160.
[15] K. Hajar, B. Guo, A. Hably, and S. Bacha, "Smart charging impact on electric vehicles in presence of photovoltaics," pp. 643–648, 2021, doi: 10.1109/icit46573.2021.9453600.
[16] H.R. Galiveeti, A.K. Goswami, N.B. Dev Choudhury, Impact of plug-in electric vehicles and distributed generation on reliability of distribution systems, Eng. Sci. Technol. Int. J. 21 (1) (Feb. 2018) 50–59, https://doi.org/10.1016/J.JESTCH.2018.01.005.

[17] Y.O. Udoakah, H.B. Sonder, L. Cipcigan, Low voltage distribution network simulation and analysis for electric vehicle and renewable energy integration, in: 2021 IEEE Power and Energy Society Innovative Smart Grid Technologies Conference, ISGT 2021, Feb. 2021, https://doi.org/10.1109/ISGT49243.2021.9372184.
[18] H.B. Sonder, L. Cipcigan, C.U. Loo, Using electric vehicles and demand side response to unlock distribution network flexibility, in: 2019 IEEE Milan PowerTech, PowerTech 2019, Jun. 2019, https://doi.org/10.1109/PTC.2019.8810521.
[19] A.R. Bhatti, Z. Salam, and R.H. Ashique, "Electric vehicle charging using photovoltaic based microgrid for remote islands," Energy Procedia, vol. 103, no. April, pp. 213–218, 2016, doi: 10.1016/j.egypro.2016.11.275.
[20] Q. Hoarau, Y. Perez, Interactions between electric mobility and photovoltaic generation: a review, Renew. Sustain. Energy Rev. 94 (Oct. 2018) 510–522, https://doi.org/10.1016/J.RSER.2018.06.039.
[21] R. Kushwaha, B. Singh, A power quality improved EV charger with bridgeless cuk converter, IEEE Trans. Ind. Appl. 55 (5) (Sep. 2019) 5190–5203, https://doi.org/10.1109/TIA.2019.2918482.
[22] Z. Ding, J. Guo, K. Lai, W.J. Lee, Spatial-temporal demand management and benefit allocation for geo-distributed charging station and EV aggregators, IEEE Trans. Ind. Appl 56 (6) (Nov. 2020) 6238–6249, https://doi.org/10.1109/TIA.2020.3024268.
[23] V. Gupta, S.R. Konda, R. Kumar, B.K. Panigrahi, Electric vehicle driver response evaluation in multiaggregator charging management with EV routing, IEEE Trans. Ind. Appl 56 (6) (Nov. 2020) 6914–6924, https://doi.org/10.1109/TIA.2020.3017563.
[24] B. Khokhar, K.P.S. Parmar, A novel adaptive intelligent MPC scheme for frequency stabilization of a microgrid considering SoC control of EVs, Appl. Energy 309 (Mar. 2022), https://doi.org/10.1016/j.apenergy.2021.118423.
[25] Khokhar B., Dahiya S., and Parmar K.P.S., "Load frequency control of a multi-microgrid system incorporating electric vehicles," 10.1080/15325008.2022.2049648, vol. 49, no. 9–10, pp. 867–883, 2022, doi: 10.1080/15325008.2022.2049648.
[26] L. Aldieri, J. Grafström, C.P. Vinci, The effect of marshallian and jacobian knowledge spillovers on jobs in the solar, wind and energy efficiency sector, Energies (Basel) 14 (14) (Jul. 2021), https://doi.org/10.3390/en14144269.
[27] F. Dell'Anna, Green jobs and energy efficiency as strategies for economic growth and the reduction of environmental impacts, Energy Policy 149 (Feb. 2021), https://doi.org/10.1016/j.enpol.2020.112031.
[28] K.A. Collett, M. Byamukama, C. Crozier, and M. Mcculloch, "Energy and transport in Africa and South Asia," pp. 1–35, 2020.
[29] J. Bajpai, J. Bower, A road map for e-mobility rransition in Rwanda - policy brief, Igc (April) (2020).
[30] K.A. Collett, S.A. Hirmer, H. Dalkmann, C. Crozier, Y. Mulugetta, M.D. McCulloch, Can electric vehicles be good for Sub-Saharan Africa? Energy Strat. Rev. 38 (July) (2021), 100722 https://doi.org/10.1016/j.esr.2021.100722.
[31] S. Bimenyimana, et al., Integration of microgrids and electric vehicle technologies in the national grid as the key enabler to the sustainable development for Rwanda, Int. J. Photoenergy 2021 (2021), https://doi.org/10.1155/2021/9928551.
[32] V. Botelho, Estimating the economic impacts of power supply interruptions, Energy Econ. 80 (May 2019) 983–994, https://doi.org/10.1016/j.eneco.2019.02.015.
[33] Rwanda Energy Group, Rwanda least cost power development plan (LCPDP) 2019-2040, Rwanda Energy Group (June) (2019) 37.
[34] "REPUBLIC OF RWANDA MINISTRY OF INFRASTRUCTURE," 2018.
[35] A. Wüest, L. Jarc, H. Bürgmann, N. Pasche, M. Schmid, Methane formation and future extraction in Lake Kivu. Lake Kivu: Limnology and Biogeochemistry of a Tropical Great Lake, Springer, Netherlands, 2012, pp. 165–180, https://doi.org/10.1007/978-94-007-4243-7_10.
[36] Karekezi, S., McDade, S., Boardman, B., Kimani, J., Lustig, N. (2012). Energy, Poverty, and Development. In Global Energy Assessment Writing Team (Author), Global Energy Assessment: Toward a Sustainable Future (pp. 151-190). Cambridge: Cambridge University Press. Available: https://iiasa.ac.at/web/home/research/Flagship-Projects/Global-Energy-Assessment/GEA_Chapter2_development_hires.pdf (accessed Jun. 19, 2021).
[37] Load flow analysis. (1974). https://www.ipsa-power.com/modules/load-flow/ (accessed Dec. 22, 2022).
[38] C. Søndergren, C. Bang, C. Hay, M. Togeby, Electric vehicles in future market models,", Grid Integr.f Electr. Vehicles Open Electr Markets (2013) 54–81, https://doi.org/10.1002/9781118568040.ch3.
[39] G. Mohy-Ud-Din, K.M. Muttaqi, D. Sutanto, Adaptive and predictive energy management strategy for real-time optimal power dispatch from VPPs integrated with renewable energy and energy storage, IEEE Trans. Ind. Appl. 57 (3) (2021) 1958–1972, https://doi.org/10.1109/TIA.2021.3057356.
[40] X. Liang, Emerging power quality challenges due to integration of renewable energy sources, IEEE Trans. Ind. Appl. 53 (2) (2017) 855–866, https://doi.org/10.1109/TIA.2016.2626253.
[41] S.G. Kwak, J.H. Kim, Central limit theorem: the cornerstone of modern statistics, Korean J. Anesthesiol. 70 (2) (Apr. 2017) 144–156, https://doi.org/10.4097/kjae.2017.70.2.144.
[42] H. Fischer, The History of the Central Limit Theorem: From Classical to Modern Probability Theory, Springer New York Dordrecht Heidelberg London, New York, 2010, https://doi.org/10.1007/978-0-387-87857-7.
[43] Y. Filmus, *Two proofs of the central limit theorem*. 2010. Accessed: Nov. 28, 2021. [Online]. Available: http://www.cs.toronto.edu/yuvalf/CLT.pdf.
[44] A. Briones, J. Francfort, P. Heitmann, M. Schey, S. Schey, J. Smart, "Vehicle-to-Grid (V2G) power flow regulations and building codes review by the AVTA," 2012, Accessed: Dec. 22, 2022. [Online]. Available: http://www.inl.gov.
[45] M.E. Hajiabadi, H.R. Mashhadi, Analysis of the probability distribution of LMP by central limit theorem, IEEE Transactions on Power Systems 28 (3) (2013) 2862–2871, https://doi.org/10.1109/TPWRS.2013.2252372.
[46] S. Zhang and R.J. Karunamuni, "On nonparametric density estimation at the boundary *," Gordon and Breach Science Publishers, 2007. doi: 10.1080/10485250008832805.
[47] "Ministry of Infrastructures, Strategic Transport Plan for EDPRS2, Kigali, 2018.
[48] Rwanda Today, "Power grid needs $54 m upgrade to curb wastage - Rwanda today," 2019. https://rwandatoday.africa/news/4383214-5062222-thjgh4z/index.html (accessed Dec. 14, 2021).
[49] V. Ajjarapu, C. Christy, The continuation power flow: a tool for steady state voltage stability analysis, IEEE Trans. Power Syst. 7 (1) (1992) 416–423, https://doi.org/10.1109/59.141737.
[50] "ANSI/IEEE Std C57.12.80-1978 : IEEE standard terminology for power and distribution transformers.," 1978.
[51] L.J. Powell, A new standard for instrument transformer applications in industry, IEEE Trans. Ind. Appl. 47 (1) (Jan. 2011) 301–305, https://doi.org/10.1109/TIA.2010.2090849.
[52] C.A. Helfrich, R.W. Carlson, Using insulation aging to size transformers in high-ambienterature secondary-selective applications, IEEE Trans. Ind. Appl. 50 (2) (2014) 1503–1508, https://doi.org/10.1109/TIA.2013.2290896.
[53] B. Sarlioglu, C.T. Morris, D. Han, S. Li, Driving toward accessibility: a review of technological improvements for electric machines, power electronics, and batteries for electric and hybrid vehicles, IEEE Ind. Appl.s Magaz. 23 (1) (Jan. 2017) 14–25, https://doi.org/10.1109/MIAS.2016.2600739.
[54] S. Satarworn, N. Hoonchareon, Impact of EV home charger on distribution transformer overloading in an urban area, in: ECTI-CON 2017 - 2017 14th International Conference on Electrical Engineering/Electronics, Computer, Telecommunications and Information Technology, 2017, pp. 469–472, https://doi.org/10.1109/ECTICon.2017.8096276.
[55] J. Liu, X. Fan, D. Li, R. Qu, H. Fang, Minimization of AC copper loss in permanent magnet machines by transposed coil connection, IEEE Trans. Ind. Appl. 57 (3) (2021) 2460–2470, https://doi.org/10.1109/TIA.2021.3066966.
[56] B. Wang, P. Dehghanian, S. Wang, M. Mitolo, Electrical safety considerations in large-scale electric vehicle charging stations, IEEE Trans. Ind. Appl. 55 (6) (2019) 6603–6612, https://doi.org/10.1109/TIA.2019.2936474.
[57] Rwanda Energy Group, "Annual report for Rwanda energy group for the year 2021-2022," Jun. 2022.